JOURNAL OF CATALYSIS 41, 51–60 (1976)

A Molecular Orbital Study of Insertion Reactions in Hydro-Platinum(II) Complexes

D. R. ARMSTRONG, R. FORTUNE, AND P. G. PERKINS

Department of Pure and Applied Chemistry, University of Strathclyde, Glasgow G1 1XL

Received April 24, 1975

The reaction mechanisms for selected insertion processes involving the hydrido-platinum(II) complex *trans*-$Pt(PH_3)_2HCl$ have been studied by an all-valence-electron molecular orbital method. Optimized reaction coordinates have been elucidated for the insertion of CS_2, CO_2, and C_2H_4 into the metal–hydrogen bond and the results correlated with available experimental data. Following the entry of the reacting ligand into the coordination sphere of the metal, transition state and subsequent product formation appear to be largely dependent on steric effects. The sensitivity of the activation energies for reaction to specific ligands is rationalized in terms of the bonding patterns associated with the different ligands.

INTRODUCTION

Systematic experimental study of ligand insertion processes in reactions involving organometallic species has resulted in a diverse range of insertion reactions being discovered (*1,2*). The majority of these insertion reactions occurs with metal complexes of the second and third transition series and the catalytic behavior exhibited by many such systems enhances their potential importance. Complexes of the heavier metals of the nickel triad are particularly interesting in this respect and, although metal–carbon bonds provide the predominant source of insertion reactions, a number of ligand insertions involving metal–hydrogen bonds have been documented.

Despite this growing interest in insertion reactions, corresponding theoretical investigation has been limited (*3*). We have previously advanced a molecular orbital description of the Wacker process (*4*), an insertion reaction where simultaneous hydrogen migration takes place. In this work we now attempt a theoretical analysis of insertions into the Pt–H bond, and the three representative reactions outlined below were selected for detailed study.

$$trans\text{-}Pt(PR_3)_2HCl + CS_2 \rightarrow trans\text{-}Pt(PR_3)_2(CS_2H)Cl \quad (1)$$

$$trans\text{-}Pt(PR_3)_2HCl + CO_2 \rightarrow trans\text{-}Pt(PR_3)_2(CO_2H)Cl \quad (2)$$

$$trans\text{-}Pt(PR_3)_2HCl + C_2H_4 \rightarrow trans\text{-}Pt(PR_3)_2(C_2H_5)Cl. \quad (3)$$

METHOD

The molecular orbital (MO) method previously applied to platinum (*5*) and palladium (*4*) complexes has been used in all the present calculations. To conserve calculation time it is expedient to replace the PR_3 ligand, where R is normally an alkyl or aryl group, by PH_3; previous calculations (*5*) indicate that no significant changes in other parts of the molecule are induced by heuristic approximations of this type. A square-planar pseudo-D_{4h} molecular geometry lying in the xy plane was assumed for both reactant and product.

Metal–ligand bond lengths were taken from previous papers (*6*) and the remaining

internuclear distances were extracted from Refs. (*1*) and (*7*).

The insertion of carbon disulphide, CS_2, into the platinum–hydrogen bond is postulated (*8*) to occur via a four-center intermediate of type B (Fig. 1) following initial formation of the five-coordinate complex A. The latter results from addition of the entering ligand at the solvent sites either above or below the molecular plane. Since carbon disulphide itself is the solvent (*8*), no theoretical problems of ligand displacement arise. Unidentate coordination of CS_2 in the manner shown in complex A has previously been suggested for a similar rhodium complex (*9*) and the present calculations on the analogous Pt system confirm the preferential formation of a platinum–sulphur bond. Of particular interest here, however, is the nature of the transition state. While experimental evidence is unable to elucidate the structure of the envisaged transition state, molecular orbital theory is capable of giving a description of both the geometric and electronic structure of any such intermediate.

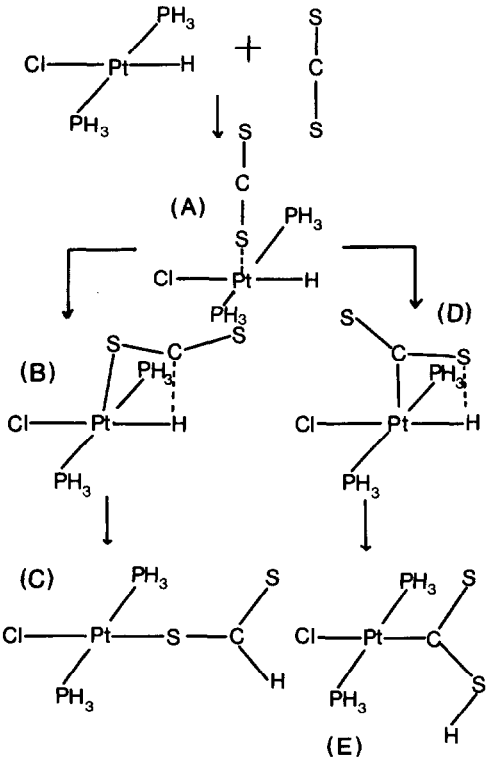

FIG. 1. Reaction sequences for CS_2 insertions.

Hypothetically, CS_2 insertion may result in either of two products (*8*), C and E, and possible transition states leading to these products are shown in Fig. 1, which demonstrates the overall reaction sequences. Unfortunately, because of the very many degrees of freedom involved, complete optimization of the transition-state geometry would take an immense amount of computer time. However, we can reduce the problem by assuming a reasonable general geometry for the transition state. Therefore, using equilibrium bond distances, restricting the CS_2 moiety to the xz plane, and acquiring the two most important parameters, the S–Ĉ–S and C–P̂t–H angles, by optimization, a reasonable transition-state geometry is obtained.

RESULTS AND DISCUSSION

Before discussing the reaction coordinates in detail, it is pertinent to examine more closely the nature of these transition states and their corresponding products. Experimental evidence favors the formation of product C, and this may be readily rationalized by comparison with related reactions (*10,11*). The calculations are in accord with this observation, product C being preferred on energy grounds. More important, however, is the theoretical prediction of a lower energy path via transition state B than via D. Since the assumption of the transition state is undoubtedly the rate-determining step, this result verifies the proposed reaction scheme. It is not difficult to trace the underlying reason for the additional stability of transition state B.

Carbon disulphide is known to act as a π-bonding bidentate ligand. The structure of the complex $Pt(PH_3)_2(CS_2)$ has been determined (*12*) and the SĈS angle shown to be 136°. Moreover, spectral measurements

on free CS_2 (*13*) demonstrate the presence of an electronically excited state of C_{2v} symmetry in which the $\hat{SCS}$ angle is 136°: This contrasts with the linear geometries of the ground state.

This correlation between excited-state and coordinated geometries implies the operation of a σ–π synergic reinforcement mechanism, with significant back-donation of electron density from the metal atom to the carbon–sulphur π^* orbitals (*1*). Furthermore, explicit calculation shows that the relevant excited-state energies decrease as the SCS angle is reduced from 180° to 120°. Consequently, in both possible transition states, the CS_2 ligand deviates from linearity, thereby alleviating some of the structural strain imposed by transition-state formation, in addition to strengthening the metal–ligand bonding as outlined above. We estimate the $\hat{SCS}$ interbond angles to be approximately 150° and 120° in B and D, respectively. In the free CS_2 molecule, the total sulphur *d*-orbital population is found to be 0.15 and the carbon–sulphur bond index (*14*) is 1.95. Inspection of Tables 1 and 2 shows sulphur *d*-orbital involvement in the bonding, as evidenced by the significant increase in electronic population and the concomitant decrease by coordination. Thus, both transition states are stabilized by this σ–π mutual reinforcement mechanism. The increased internuclear repulsion energy in transition state D brings about severe geometric distortion of the coordinated ligand: This, however, proves insufficient to lower the energy of this transition state below that of B.

1. Reaction (1), CS_2 Insertion

In general, for simplicity the reaction coordinates were constructed by systematically changing relevant bond angles and

TABLE 1A

THE ELECTRONIC DISTRIBUTION IN REACTION 1 LEADING TO PRODUCT (C)

	Pt	P	Cl	H	C	S_1	S_2
A	+0.257	−0.112	−0.432	−0.179	+0.221	−0.072	−0.082
1	+0.263	−0.114	−0.429	−0.181	+0.220	−0.068	−0.086
2	+0.274	−0.115	−0.424	−0.183	+0.214	−0.066	−0.098
3	+0.288	−0.115	−0.416	−0.180	+0.198	−0.067	−0.113
B	+0.253	−0.122	−0.379	−0.086	+0.246	−0.148	−0.158
1	+0.243	−0.102	−0.315	−0.132	+0.240	−0.184	−0.195
2	+0.223	−0.092	−0.361	−0.089	+0.203	−0.174	−0.197
3	+0.235	−0.097	−0.377	−0.008	+0.151	−0.185	−0.203
4	+0.269	−0.100	−0.372	+0.046	+0.115	−0.224	−0.219
5	+0.299	−0.101	−0.366	+0.067	+0.110	−0.263	−0.233
C	+0.316	−0.101	−0.358	+0.065	+0.109	−0.283	−0.239
	Pt–P	Pt–Cl	Pt–H	S_1–C	S_2–C	Pt–S	C–H
A	0.531	0.516	0.567	0.131	1.911	1.975	0.000
1	0.524	0.517	0.557	0.148	1.910	1.960	0.001
2	0.515	0.522	0.544	0.163	1.936	1.907	0.002
3	0.503	0.531	0.529	0.197	1.953	1.838	0.002
B	0.504	0.577	0.440	0.311	1.783	1.723	0.143
1	0.532	0.685	0.351	0.330	1.692	1.692	0.243
2	0.495	0.635	0.163	0.614	1.448	1.711	0.544
3	0.489	0.597	0.083	0.661	1.374	1.681	0.689
4	0.498	0.597	0.052	0.627	1.325	1.657	0.786
5	0.507	0.604	0.029	0.569	1.289	1.643	0.851
C	0.514	0.618	0.021	0.532	1.247	1.671	0.870

TABLE 1B
PARTIAL BOND INDICES

	Pt(*s*)–S_1	p_x–S_1	p_y–S_1	p_z–S_1	$d_{x^2-y^2}$–S_1	d_{xz}–S_1	d_{z^2}–S_1	d_{yz}–S_1	d_{xy}–S_1
A	0.038	0.009	0.008	0.061	0.001	0.003	0.011	0.002	0.000
1	0.051	0.009	0.009	0.052	0.002	0.006	0.014	0.004	0.000
2	0.055	0.007	0.010	0.047	0.004	0.013	0.017	0.009	0.001
3	0.051	0.006	0.010	0.049	0.009	0.021	0.032	0.017	0.003
B	0.089	0.015	0.010	0.062	0.028	0.023	0.049	0.026	0.008
1	0.116	0.037	0.011	0.062	0.021	0.020	0.026	0.026	0.010
2	0.098	0.053	0.014	0.062	0.246	0.057	0.051	0.019	0.015
3	0.109	0.044	0.015	0.051	0.303	0.072	0.032	0.014	0.019
4	0.118	0.036	0.017	0.043	0.302	0.051	0.028	0.010	0.020
5	0.121	0.022	0.019	0.035	0.276	0.028	0.034	0.007	0.024
C	0.125	0.016	0.020	0.034	0.251	0.018	0.038	0.006	0.025
	S_1(*s*)–Pt	p_x–Pt	p_y–Pt	p_z–Pt	$d_{x^2-y^2}$–Pt	d_{xz}–Pt	d_{z^2}–Pt	d_{yz}–Pt	d_{xy}–Pt
A	0.075	0.009	0.008	0.021	0.000	0.003	0.013	0.002	0.000
1	0.078	0.011	0.009	0.021	0.000	0.008	0.016	0.004	0.000
2	0.078	0.012	0.010	0.019	0.001	0.015	0.018	0.009	0.001
3	0.078	0.015	0.011	0.031	0.004	0.023	0.017	0.016	0.003
B	0.072	0.019	0.013	0.133	0.008	0.019	0.015	0.023	0.009
1	0.062	0.021	0.017	0.156	0.013	0.011	0.020	0.017	0.013
2	0.144	0.084	0.017	0.299	0.015	0.006	0.019	0.015	0.016
3	0.180	0.107	0.017	0.283	0.014	0.007	0.022	0.012	0.019
4	0.202	0.137	0.019	0.200	0.009	0.010	0.019	0.009	0.022
5	0.219	0.174	0.021	0.092	0.005	0.015	0.014	0.006	0.023
C	0.234	0.180	0.022	0.035	0.003	0.018	0.011	0.006	0.024

distances involving the ligand as the system moved along the reaction path. All other Pt–X bond distances were kept constant. The reaction coordinates for CS_2 insertion resulting in products C and E are depicted graphically in Figs. 2 and 3, respectively. Both reaction sequences are initiated by platinum–sulphur bond formation. The calculations suggest that the CS_2 ligand is loosely bound to the metal complex, via the sulphur atom, at a distance of 0.4 nm (i.e., complex A). This situation militates against a path leading to product E, since the necessary Pt–C bond formation requires this Pt–S bond to be broken. In both transition states the metal–

TABLE 1C
TOTAL *d*-ORBITAL OCCUPANCIES

	Pt	P	Cl	S_1	S_2
A	8.818	0.321	0.106	0.192	0.149
1	8.830	0.329	0.107	0.224	0.150
2	8.841	0.341	0.109	0.279	0.152
3	8.834	0.355	0.112	0.358	0.159
B	8.754	0.375	0.120	0.414	0.178
1	8.702	0.364	0.125	0.421	0.171
2	8.823	0.342	0.115	0.433	0.170
3	8.847	0.336	0.109	0.427	0.171
4	8.814	0.336	0.109	0.397	0.172
5	8.756	0.336	0.109	0.361	0.172
C	8.764	0.335	0.110	0.341	0.181

TABLE 2
THE ELECTRONIC DISTRIBUTION IN REACTION 1 LEADING TO PRODUCT (E)

	Pt	P	Cl	H	O	S_1	S_2
A	+0.257	−0.112	−0.432	−0.179	+0.221	−0.072	−0.082
1	+0.287	−0.111	−0.407	−0.141	+0.181	−0.074	−0.145
2	+0.337	−0.109	−0.399	−0.106	+0.038	−0.044	−0.171
3	+0.299	−0.119	−0.382	−0.084	+0.046	−0.032	−0.151
D	+0.259	−0.126	−0.369	−0.081	+0.157	−0.074	−0.168
1	+0.253	−0.126	−0.349	−0.078	+0.116	−0.180	−0.043
2	+0.249	−0.116	−0.316	−0.094	+0.055	−0.204	−0.000
3	+0.262	−0.103	−0.336	−0.084	+0.014	−0.219	+0.004
4	+0.268	−0.106	−0.361	−0.047	+0.029	−0.220	−0.029
5	+0.268	−0.106	−0.372	+0.006	+0.029	−0.230	−0.068
E	+0.274	−0.106	−0.375	+0.024	+0.033	−0.236	−0.094
	Pt–P	Pt–Cl	Pt–H	Pt–C	S_1–C	S_2–C	S_1–H
A	0.531	0.516	0.567	0.015	1.911	1.975	0.007
1	0.540	0.544	0.518	0.110	1.906	1.833	0.106
2	0.489	0.549	0.448	0.114	1.812	1.696	0.199
3	0.513	0.585	0.405	0.099	1.729	1.714	0.269
D	0.526	0.582	0.456	0.204	1.658	1.665	0.223
1	0.523	0.624	0.417	0.192	1.681	1.592	0.278
2	0.534	0.688	0.347	0.172	1.692	1.454	0.385
3	0.506	0.688	0.177	0.288	1.659	1.247	0.683
4	0.484	0.649	0.103	0.378	1.651	1.215	0.813
5	0.481	0.629	0.062	0.423	1.646	1.189	0.889
E	0.485	0.626	0.048	0.438	1.616	1.165	0.914

hydrogen bond distance is assumed to be unperturbed by the entering ligand, subsequent insertion occurring via hydrogen migration, as shown. These two reaction sequences will now be considered in greater depth.

The electronic properties associated with CS_2 insertion to give product C are summarised in Table 1. In addition to electronic populations and total bond indices, we make use of a partial bond index de-

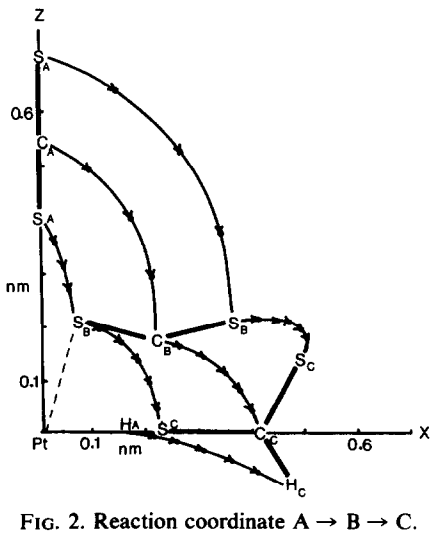

FIG. 2. Reaction coordinate A → B → C.

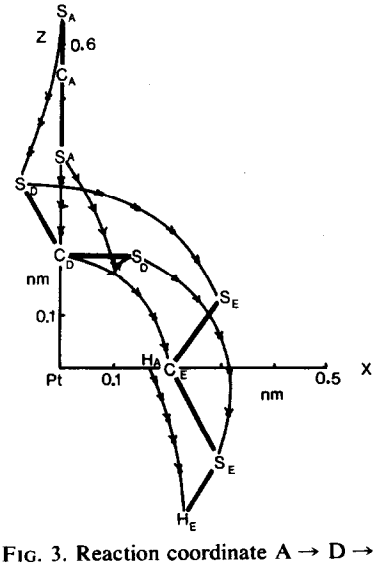

FIG. 3. Reaction coordinate A → D → E.

fined by

$$P_{\lambda B} = \sum_{\sigma \text{ on } B} P^2_{\lambda\sigma},$$

where $P_{\lambda\sigma}$ is the density matrix element between atomic orbitals λ and σ on atoms A and B, respectively. In this way the contribution of a particular orbital λ to the total interatomic bonding may be assessed. Clearly, summation of these partial bond indices must lead to the total bond index

$$P_{AB} = \sum_{\lambda \text{ on } A} \sum_{\sigma \text{ on } B} P^2_{\lambda\sigma}.$$

The increased coordination number of Pt arising from CS_2 attachment results in decreased metal–ligand interaction in the parent complex $Pt(PH_3)_2HCl$. However, experimental data derived from infrared spectra can be interpreted as meaning that formation of an intermediate of type A increases the metal–hydrogen bond strength over that in the parent complex and this is attributable to an increase in metal oxidation state (*8*). Conversely, the calculations predict a marginal weakening in this bond. However, it is impossible to ascertain the extent of the influence of the nonseparable mass-effects of the other ligands in the complex and the marginal change in platinum–hydrogen bond index incurred through platinum–sulphur bonding should not be interpreted as necessarily opposing experimental evidence.

Formation of transition state B is facilitated by increased metal–sulphur bonding, which offsets in part the increased nuclear repulsion energy. Occupation of the π^* anti-bonding orbitals of the CS_2 ligand is accompanied by a decreased C–S bond index. The σ-donor capabilities of this ligand, characteristic of this type of bonding, is evident from the electronic polarization of the CS_2 moiety toward the metal complex. In contrast with S_2, which does not participate directly in metal–ligand bonding, the *d*-orbital population of S_1 increases markedly with the degree of coordination. Inspection of the partial bond indices (Table 1) shows that the p_z orbital of S_1, being primarily responsible for the ligand σ-donor properties, plays an important role in Pt–S bond formation. At this stage of the process the diffuse platinum *s* orbital also contributes extensively to the overall bonding. It is also noteworthy that, in the transition state, there is direct C–H bonding (which reduces the Pt–H bond index) and, hence, the system may be considered as a "four-center" intermediate of the type suggested by Palazzi *et al.* (*8*). Consistent with this, the total energy data show that formation of the labile intermediate B constitutes the activation energy barrier.

Product formation appears to take place with hydrogen migration permitting complete CS_2 insertion. The decreasing Pt–H and S_1–C bonding is offset by increasing Pt–S_1 and C–H interactions, the net result being energetically favored. As the CS_2 ligand approaches the *x*-axis (Fig. 1), the importance of the metal $d_{x^2-y^2}$ orbital is enhanced and Pt–S bonding in the product is governed by interactions with this orbital. In a similar manner, the S_1 *s*-orbital contribution to the Pt–S_1 bond takes over the role of the previously dominant S_1 *p* orbital. Also, while the S_1–C bond becomes essentially single, the S_2–C bond retains much of its double-bond character. Electron-density contour maps for the reaction (Fig. 4) bring out this point well.

The alternative product, E, resulting from CS_2 insertion, requires assumption of a transition state of type D. Here, direct Pt–C bonding replaces the Pt–S interaction found in the initial complex A. This, in addition to the less favorable steric commitments imposed by such a transition state, precludes the formation of product E. Nevertheless, it is instructive to examine briefly the reaction coordinate shown in Fig. 3. Inspection of Table 2 shows that the transition state is achieved by S_2–H and Pt–C bond formation at the expense of

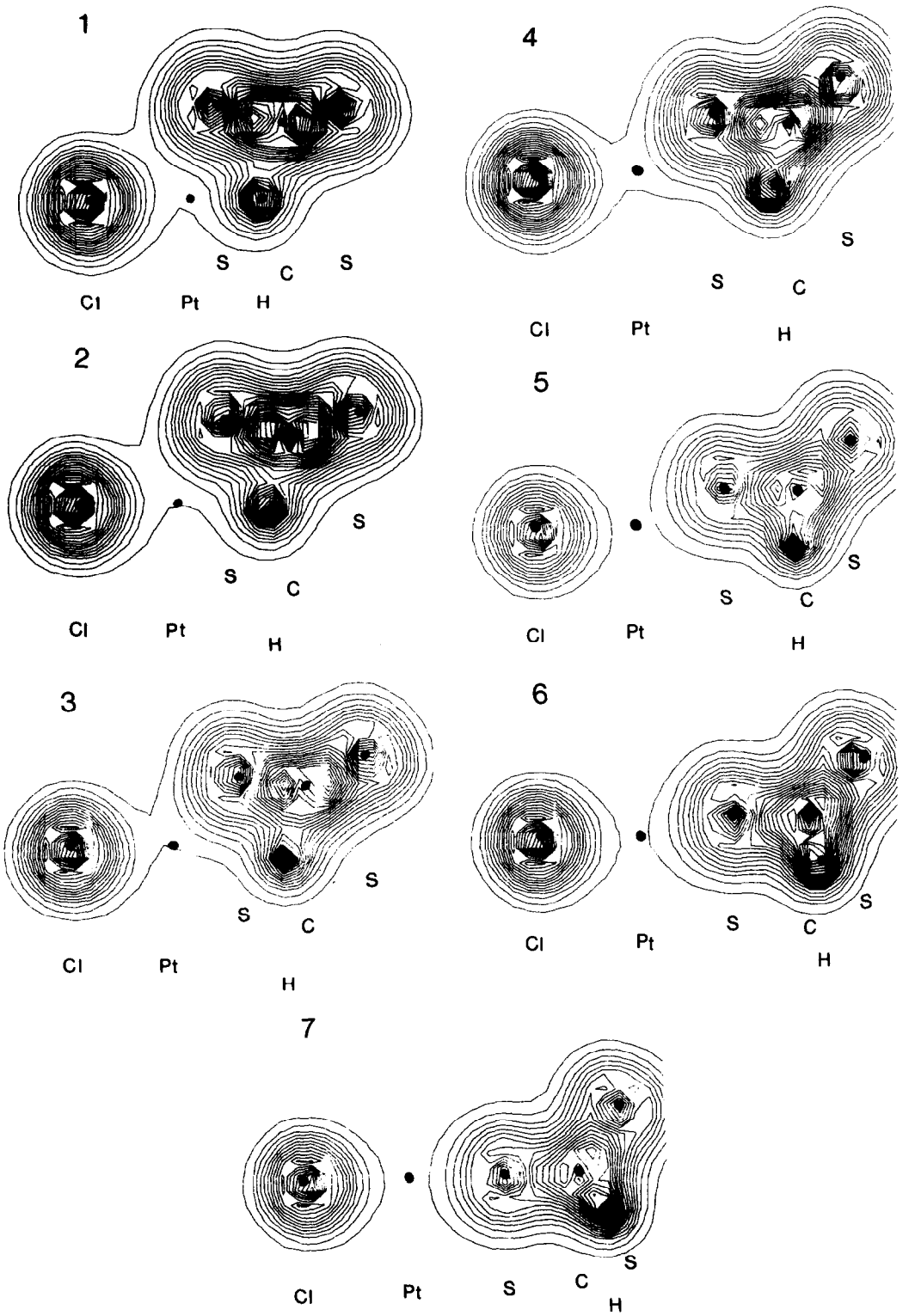

FIG. 4. Electron density contours for CS_2 insertion.

Pt–H and C–S bonds. The strong distortion of the CS_2 ligand leads to distinctly weaker C–S bonding compared with transition state B. Also, the Pt–C bonding is weaker (i.e., the associated bond index is far lower) than the comparable Pt–S bonding, indicating the relative instability of transition state D. Retention of double-bond character for $C–S_1$, together with the single-bond nature of $C–S_2$, is rather similar to that found in the previous process. The increase in Pt–Cl bond index and the decrease in Pt–P bond index are also manifest in both reaction sequences. It may, therefore, be concluded that the $Cl–Pt(PH_3)_2$ moiety does not exert a major influence in product determination, the nuclear repulsions dictating the course of the reaction.

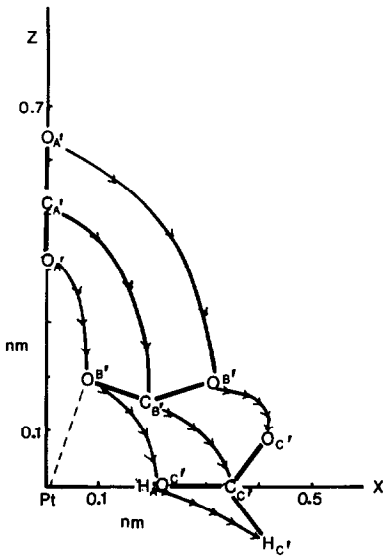

FIG. 5. Reaction coordinate for CO_2 insertion.

2. *Reaction (2), CO_2 Insertion*

Although the analogous insertion of CO_2 into a platinum–hydrogen bond has not been reported, this ligand is known to insert into certain metal–carbon bonds (*15*). It is therefore of interest to compare CO_2 and CS_2 insertion into the Pt–H bond. The transition state was optimised as before by varying θ and ϕ and the electronic proper-

TABLE 3
THE ELECTRONIC DISTRIBUTION IN REACTION 2

	Pt	P	Cl	H	C	O_1	O_2
A′	+0.272	−0.109	−0.432	−0.178	+0.502	−0.228	−0.232
1	+0.272	−0.112	−0.432	−0.183	+0.505	−0.221	−0.226
2	+0.275	−0.116	−0.432	−0.191	+0.509	−0.211	−0.217
3	+0.282	−0.122	−0.426	−0.199	+0.521	−0.217	−0.214
B′	+0.317	−0.126	−0.382	−0.083	+0.512	−0.336	−0.306
1	+0.357	−0.112	−0.312	−0.126	+0.459	−0.390	−0.319
2	+0.380	−0.121	−0.343	−0.085	+0.381	−0.372	−0.285
3	+0.379	−0.123	−0.369	−0.017	+0.316	−0.364	−0.259
4	+0.388	−0.122	−0.378	+0.018	+0.272	−0.374	−0.243
C′	+0.396	−0.122	−0.377	+0.014	+0.249	−0.375	−0.229
	Pt–P	**Pt–Cl**	**Pt–H**	**Pt–O_1**	**O_1–C**	**O_2–C**	**C–H**
A′	0.541	0.523	0.575	0.034	1.911	1.939	0.000
1	0.538	0.524	0.571	0.036	1.901	1.937	0.000
2	0.533	0.526	0.564	0.034	1.884	1.928	0.000
3	0.527	0.537	0.542	0.034	1.852	1.894	0.018
B′	0.542	0.609	0.367	0.130	1.597	1.741	0.324
1	0.539	0.729	0.259	0.149	1.457	1.749	0.487
2	0.498	0.706	0.116	0.370	1.226	1.816	0.746
3	0.495	0.658	0.063	0.434	1.120	1.842	0.862
4	0.500	0.643	0.041	0.427	1.046	1.865	0.913
C′	0.504	0.648	0.038	0.408	1.001	1.886	0.919

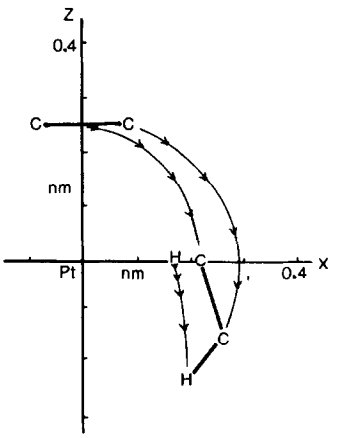

Fig. 6. Reaction coordinate for C_2H_4 insertion.

ties of the systems along the reaction coordinate A′ → B′ → C′, depicted in Fig. 5, are outlined in Table 3. It turns out that this reaction sequence is similar to the CS_2 insertion, the major differences being due to the increased ionicity of coordinated CO_2. The CO_2 ligand also deviates from linearity on coordination, the extent of the distortion being slightly greater than in the CS_2 case. The low Pt–O_2 bond index in the intermediate B′ underscores the importance of the σ–π synergic mechanism which operates in CS_2 insertions. The Pt–H bond is found to be weaker and the C–H bond stronger than in transition state B. The results also indicate that there will be a higher energy barrier to CO_2 insertion and this may account for its presently being unobserved. Subsequent product formation closely follows the CS_2 insertion, with the Pt–O bond remaining weaker than the Pt–S bond throughout the reaction. The absence of low-lying formally unoccupied *d* orbitals in oxygen and the consequent nonexistence of accessible π^* orbitals probably accounts for the observed differences between the two systems.

3. Reaction (3), C_2H_4 Insertion

A related reaction of potential importance in catalytic hydrogenation is the insertion of ethylene into the platinum–hydrogen bond (*16*). As in the case of CS insertion, the π^* orbital of ethylene allows a σ–π reinforcement mechanism (*17*), so stabilizing the transition state. The calculations show that initial coordination of ethylene at ca. 0.25 nm above the molecular plane directly generates the transition state. The subsequent reaction sequence shown in Fig. 6 necessitates the formation of a metal–carbon σ-bond. This, in conjunction with hydrogen migration, is found to be energetically favorable, formation of the penta-coordinate $Pt(PH_3)_2HCl(C_2H_4)$

TABLE 4
THE ELECTRONIC DISTRIBUTION IN REACTION 3

	Pt	P	Cl	H	C_1	C_2	
F	+0.262	−0.146	−0.457	−0.190	−0.021	−0.045	
1	+0.266	−0.148	−0.428	−0.177	−0.062	−0.022	
2	+0.261	−0.151	−0.396	−0.122	−0.157	+0.038	
3	+0.302	−0.122	−0.337	−0.009	−0.282	−0.015	
4	+0.239	−0.132	−0.395	+0.126	−0.169	−0.155	
G	+0.268	−0.128	−0.407	+0.038	−0.180	−0.095	
	Pt–P	Pt–Cl	Pt–H	C_1–C_2	C_2–H	Pt–C_1	Pt–C_2
F	0.511	0.521	0.541	1.885	0.000	0.099	0.096
1	0.507	0.547	0.519	1.842	0.049	0.119	0.099
2	0.499	0.582	0.449	1.641	0.187	0.142	0.091
3	0.499	0.709	0.133	0.949	0.754	0.324	0.127
4	0.449	0.611	0.048	0.946	0.844	0.512	0.086
G	0.468	0.595	0.041	0.983	0.916	0.516	0.062

being the rate-determining step. The electronic properties summarized in Table 4 show the expected reduction of carbon–carbon double-bond character upon initial coordination. Further destruction of the double bond accompanies Pt–C_1 and C_2–H bond formation, both occurring within narrow geometric limits.

In conclusion, it appears that insertion reactions of this type are largely dominated by internuclear repulsion energies. Any feature of the bonding which offsets this, such as a σ–π coordination mechanism, should facilitate product formation.

ACKNOWLEDGMENT

One of us (R.F.) thanks the University of Strathclyde for Crawford Bursary.

REFERENCES

1. Hartley, F. R., "The Chemistry of Platinum and Palladium." Applied Science Publishers, London, 1973.
2. Maitlis, P. M., "The Organic Chemistry of Palladium." Applied Science Publishers, London, 1973.
3. Sakaki, S., Kato, H., Kanai, H., and Tarama, K., *Bull. Chem. Soc. Jap.* **47**, 377 (1974).
4. Armstrong, D. R., Fortune, R., and Perkins, P. G., to be published.
5. Armstrong, D. R., Fortune, R., and Perkins, P. G., *Inorg. Chim. Acta* **9**, 9 (1974).
6. Zumdahl, S. S., and Drago, R. S., *J. Amer. Chem. Soc.* **90**, 6669 (1968).
7. "Interatomic Distances in Molecules and Ions," Special Publication No. 11, Chemical Society, London, 1958.
8. Palazzi, A., Busetto, L., and Graziani, M., *J. Organometal. Chem.* **30**, 273 (1971).
9. Baird, M. C., and Wilkinson, G., *J. Chem. Soc. (A)*, 865 (1967).
10. Baird, M. C., Hartwell, G., and Wilkinson, G., *J. Chem. Soc. (A)*, 2037 (1967).
11. Commereuc, D., Douek, I., and Wilkinson, G., *J. Chem. Soc. (A)*, 1771 (1970).
12. Mason, R., and Rae, A. I. M., *J. Chem. Soc. (A)*, 1765 (1970).
13. Kleman, B., *Can. J. Phys.* **41**, 2034 (1963).
14. Armstrong, D. R., Perkins, P. G., and Stewart, J. J. P., *J. C. S. Dalton*, 838 (1973).
15. Kolomnikov, I. S., Gusev, A. O., Belopotapova, T. S., Grigoryan, M. Kh., Lystak, T. V., Struchkov, Yu. T., and Vol'Pin, M. E., *J. Organometal. Chem.* **69**, C10 (1974).
16. Chatt, J., and Shaw, B. L., *J. Chem. Soc.*, 5075 (1962).
17. Chatt, J., Duncanson, L. A., and Venanzi, L. M., *J. Chem. Soc. (A)*, 4456 (1955).